

## Electrochemical Oxidation of Reactive Blue 222 on Boron-Doped Diamond Electrodes

Manuel Rangel<sup>1</sup>, José L. Nava<sup>1,\*</sup>, Juan M. Peralta-Hernández<sup>2</sup>, Gilberto Carreño<sup>1</sup>,  
Ricardo J. Guerra-Sánchez<sup>2</sup>

<sup>1</sup> Universidad de Guanajuato, Departamento de Ingeniería Geomática e Hidráulica, Guanajuato, Guanajuato, C.P. 36000, México.

<sup>2</sup> Centro de Innovación Aplicada en Tecnologías Competitivas (CIATEC), Departamento de Investigación Ambiental, León, Guanajuato, C.P. 37545, México.

\*E-mail: [jlnm@ugto.mx](mailto:jlnm@ugto.mx)

Received: 4 December 2012 / Accepted: 2 February 2013 / Published: 1 March 2013

---

Electrochemical oxidation of reactive blue 222 (1.6 mM, 1300 mg dm<sup>-3</sup> COD) in 0.5 M Na<sub>2</sub>SO<sub>4</sub> aqueous media (which resembles a textile wastewater) on a boron-doped diamond electrode (BDD) was studied, using bulk electrolysis. The influence of current density and hydrodynamics was investigated. The degradation rate depends on current density and with hydrodynamics. Generated carboxylic acids such as ascorbic, oxalic, benzoic, citric, fumaric and maleic were detected and quantified by HPLC measures. The electrolysis with a BDD electrode at 20 mA cm<sup>-2</sup> and mean linear flow velocity of 146 cm s<sup>-1</sup> was the only experiment that led to 100% mineralization of reactive blue 222, with an energy consumption of 11.8 KWh m<sup>-3</sup> and fractional integral current efficiency of 0.7.

---

**Keywords:** Degradation of organics, Boron-doped diamond electrode, Reactive blue 222, Electrochemical oxidation.

### 1. INTRODUCTION

Although the textile industry plays an important role in the world economy and our daily life, it also consumes a large quantity of water (up to 150 L of water to dye 1 kg of cotton) and generates a huge amount of wastewater [1]. Textile effluents are one of the most difficult to treat wastewaters on account of their considerable amount of suspended solids and of their high chemical oxygen demand (COD) due to the massive presence of weakly biodegradable and often toxic substances such as additives, detergents, surfactants and dyes.

Given the great variety of fibres, dyes, process aids and finishing products used, dyed wastewaters display a great chemical complexity and diversity which are not adequately treated in

conventional wastewater treatment plants. Therefore, dyes and their derivatives often accumulate in the environment [2].

Different treatment processes, such as chemical coagulation [3], electrocoagulation [3,4], activated carbon, adsorption [5] and ultrafiltration [6], have been proposed in the literature to effectively treat textile wastewater. However, all these options lead to the removal of the dye from wastewater and its relocation elsewhere.

Another approach to textile wastewater treatment is represented by biological processes [2], Fenton treatment [7], and ozonation [8]; these reports focus on oxidizing organic matter at low concentration and reported efficiencies are poor. Electrochemical incineration is a technique that has been found adequate for the treatment of colored wastewaters. Recently, several researches have shown that BDD electrodes exhibit good performance, since a large amount of hydroxyl radical ( $\bullet\text{OH}$ ) are formed by water oxidation on the electrode surface [9, 10, 11]. The hydroxyl radical exhibits strong oxidant properties by which complex color molecules are degraded to  $\text{CO}_2$ . BDD anodes have good chemical and electrochemical stability even in strong and aggressive media, with a long life and a wide potential window of water discharge. Thus BDD are promising anodes for the treatment of wastewaters containing dyes.

The aim of this work was to study the electrochemical oxidation of a wastewater model containing a very complex dye using a BDD anode. Reactive blue 222 was chosen as a model dye because it is a commercially common disazoic dye containing many aromatic rings and sulphonic groups, which make its treatment with traditional processes difficult. The impact of the main operating parameters, such as current density (lower than the limiting current of electrocombustion of organics) and flow velocity, on COD removal was investigated. The evolution of reactive blue 222 by-products, mainly carboxylic acids, followed by ion-exclusion HPLC technique, was also examined.

## 2. EXPERIMENTAL DETAILS

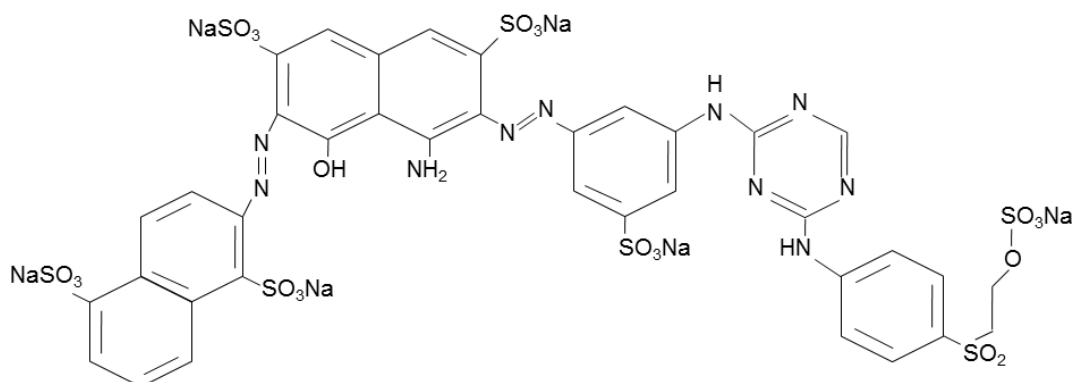


**Figure 1.** Chemical structure of reactive blue 222.

Reactive blue 222 ( $C_{38}H_{23}N_{10}Na_6O_{22}S_7$ ) solutions were prepared at  $0.04 \text{ mol dm}^{-3}$  COD ( $1300 \text{ mg dm}^{-3}$  COD) in  $0.5 \text{ mol dm}^{-3}$   $Na_2SO_4$ ; the resulting solution exhibits apH of 4.5. These solutions were prepared with analytical grade reagents and deionised water with  $18 \text{ m}\Omega^{-1} \text{ cm}^{-1}$  resistivity from a Mill-Q™ system. It is important to point out that the composition of the prepared solutions resembles a textile wastewater. The structure of reactive blue 222 is shown in Figure 1. Carboxylic acids (oxalic, citric, ascorbic, benzoic, maleic, fumaric) and organic solvents were HPLC grade from Merck and JT Baker.

## 2.1 Equipment

A DC power supply BK Precision-model-1621A was used for all electrolyses experiments. COD analyses were performed using a dry-bath Lab Line Model 2008, and a visible spectrophotometer Genesis 20. The evolution of carboxylic acids were quantified by HPLC determinations using the above LC fitted with a Phenomenex Luna C-18,  $150 \times 4.6 \text{ mm}$  column, at  $35 \text{ }^\circ\text{C}$  and selecting the photodiode detector at  $\lambda = 210 \text{ nm}$ . A  $2.5 \text{ mM}$  potassium phosphate buffer at pH 2.5, and with a flow at  $1.3 \text{ mL min}^{-1}$ , was used as mobile phase.

The cell potential was measured by the power supply. The BDD electrode potential was measured by the difference between BDD and a saturated mercurous sulphate reference electrode (SSE) (Radiometer-model-XR200),  $0.615 \text{ V vs. SHE/V}$ ; this electrode potential was detected by a high impedance multimeter (Agilent-model-34401A). All electrode potentials shown in this work are presented with regard to SHE.

The FM01-LC reactor has been described in detail in the literature [12]. An exploded view of the cell, that includes the turbulence promoter used within the cell channel, is shown in a previous communication [13]. BDD anode was 2-D (plate), while a platinum coated titanium flat sheet was used as the cathode. BDD electrodes were provided by Metakem™, with a thickness of  $2\text{-}7 \text{ }\mu\text{m}$  supported on Ti. Details on the FM01-LC cell characteristics are given in Table 1.

**Table 1.** BDD electrode dimensions, experimental details of the FM01-LC reactor.

Electrode length, L	16 cm
Electrode height, B	4 cm
Electrode spacing, S	0.55 cm
Electrode Area,	$64 \text{ cm}^2$
Overall voidage, $\varepsilon$ (using BDD and turbulence promoter)	0.83
Hydraulic (equivalent) diameter, $d_e = 2BS/(B+S)$	0.97 cm
Turbulence promoter	Plastic mesh type D <sup>a</sup> CD and <sup>b</sup> LD=11 mm.

Overall voidage is the ratio of the free space in the channel to overall channel volume.

<sup>a</sup>CD = internal dimension of shorter mesh diagonal.

<sup>b</sup> LD = internal dimension of longer mesh diagonal.

The undivided FM01-LC reactor, with a single electrolyte compartment and the electrolyte flow circuit, is shown in Figure 2.

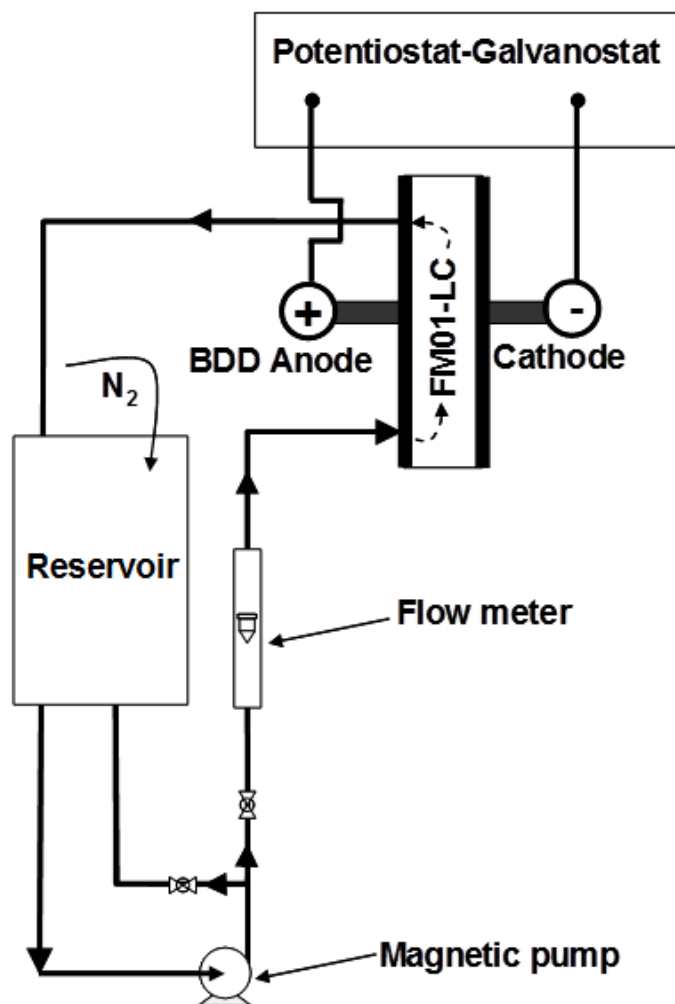


**Figure 2.** Electrical and flow circuit for the measurement of electrochemical incineration kinetics at FM01-LC reactor.

The electrolyte was contained in a 1 L polycarbonate reservoir. A magnetically coupled pump of 1/15 hp March MFG, model MDX-MT-3 was used; the flow rates were measured by a variable area glass rotameter from Cole Palmer, model F44500. The electrolyte circuit was constructed from PVC tubing with 0.5 inch diameter; the valves and the three way connectors were made of PVC.

## 2.2 Methodology for electrochemical tests

Electrochemical incinerations of reactive blue 222 were carried out in the FM01-LC cell at mean linear flow velocities between  $3.6 \leq u \leq 146 \text{ cm s}^{-1}$  and current density in the interval of  $10 \leq J \leq 20 \text{ mA cm}^{-2}$ . These current densities are located in the potential range of  $2.4 \leq E \leq 2.9 \text{ V vs. SHE}$ , where organics are oxidized by hydroxyl radicals through the reaction described by equation (1) [13]:



It is important to point out that these current densities,  $10 \leq J \leq 20 \text{ mA cm}^{-2}$ , are lower than the initial limiting current densities of electro combustion,  $J_L(t=0)$ , which was calculated at the initial chemical oxygen demand ( $\text{COD}(t=0)$ ) by means of equation (2) and reported in table 2 [14]:

$$J_L(t) = 4Fk_m\text{COD}(t) \quad (2)$$

Where  $J_L(t)$  is the limiting current density at any time of electrolysis, four is the number of exchanged electrons,  $k_m$  is the global mass transport, and  $\text{COD}(t)$  is the chemical oxygen demand at any time of electrolysis.

**Table 2.** Initial limiting current densities values of electro combustion,  $J_L(t=0)$ , and mass transport coefficients,  $k_m$ , as a function of mean linear flow velocities.  $\text{COD}(t=0) = 4 \times 10^{-5} \text{ mol dm}^{-3}$ ;  $F = 96485 \text{ C mol}^{-1}$ .

$u / \text{cm s}^{-1}$	$^a k_m / \text{cm s}^{-1} (\times 10^3)$	$^b J_L(t=0) / \text{mA cm}^{-2}$
73	10.2	160
146	15.7	246

<sup>a</sup>Determined by eq. (3).

<sup>b</sup>Determined by eq. (2).

Global mass transport coefficient in practice is usually characterized by measuring the limiting current density over a range of electrolyte velocities. The exact form of the mass transport correlation is best evaluated through an analysis of experimental data and will depend on the electrode geometry, electrochemical cell geometry, and types of fluid flows. For the purpose of this paper, the mass transport correlation was taken as [15]:

$$\frac{k_m d_e}{D} = 0.56 \left( \frac{u d_e}{\nu} \right)^{0.62} \left( \frac{\nu}{D} \right)^{0.33} \quad (3)$$

This was obtained by Griffiths et al. for the reduction process of ferricyanide to ferrocyanide ion [15]. This correlation was obtained in presence of a type D turbulence promoter that increases mass transport. The dimensions of the FM01-LC employed in this paper are showed in Table 1. The electrolyte properties such as diffusion coefficient of ferricyanide and kinematic viscosity, used for the evaluation of Equation 3, were  $D = 6.4 \times 10^{-6} \text{ cm}^2 \text{ s}^{-1}$  and  $\nu = 9.56 \times 10^{-3} \text{ cm}^2 \text{ s}^{-1}$ , respectively [15].

The incineration evolution was estimated by COD analysis of samples taken at different times. The COD values were determined by the closed reflux dichromate titration method [16]. It is important to mention that COD analyses discount interferences from the sulfur species like sulfuric and peroxodisulfuric acids. COD analysis were performed

Current efficiency for anodic oxidation of reactive blue 222 was calculated from COD values using the following relationship [13]:

$$\phi = \frac{4FV[\text{COD}(t=0) - \text{COD}(t)]}{It} \quad (4)$$

where four is the number of exchanged electrons,  $V$  is the solution volume in  $\text{cm}^3$ ,  $I$  is the intensity current applied in the electrolysis, in A, and  $t$  is the time of electrolysis (s).

### 3. RESULTS AND DISCUSSION

#### 3.1 COD removal

Applied current density effect on COD and current efficiency during reactive blue 222 electrochemical oxidation are shown in Figure 3.

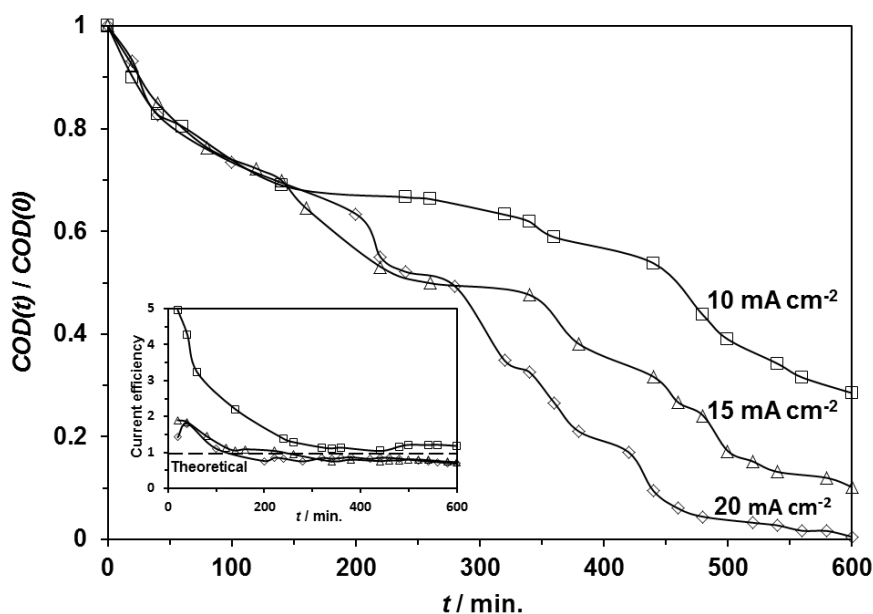
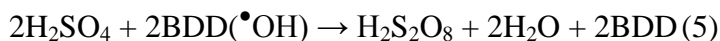


**Figure 3.** Influence of applied current density on the evolution of normalized COD and current efficiency (inset) during the electrolysis of reactive blue 222. Initial electrolyte:  $0.04 \text{ mol dm}^{-3}$  COD ( $1300 \text{ mg dm}^{-3}$   $\text{COD}(0)$ ) in  $0.5 \text{ mol dm}^{-3}$   $\text{Na}_2\text{SO}_4$ ; the resulting solution exhibits a pH of 4.5,  $T=298 \text{ K}$ . Conditions:  $u = 146 \text{ cm s}^{-1}$ ,  $A = 64 \text{ cm}^2$ . Current densities are shown in the Figure.

As can be observed the normalized COD is independent of current density at  $t < 150$  minutes, and at  $t > 150$  minutes, normalized COD decreases as a function of current density. Total COD removal is only obtained under current density condition of  $20 \text{ mA cm}^{-2}$ , indicating complete dye mineralization. This last is attributed to the reaction of organics with electro-generated  $\bullet\text{OH}$  radicals.

Nevertheless, the oxidation of organics with  $\bullet\text{OH}$  radicals is not the only oxidation mechanism occurring on BDD. Indeed, peroxodisulphuric acid is also produced in solutions containing sulphates in acidic media, during electrolysis with BDD electrodes (Eq. 5) [9, 11, 13]:



Peroxodisulphuric acid is also a very strong oxidant agent, which use to increase the COD removal rate.

From the analysis of Figure 3 (inset), it can be also observed that an increase in current density results in a decrease in current efficiency. The higher current efficiency than the theoretical, for  $10 \text{ mA cm}^{-2}$ , suggests that reactive blue oxidation by-products help the degradation itself [17]. A similar behavior occurred for 15 and  $20 \text{ mA cm}^{-2}$ , at  $t < 180$  minutes of electrolysis, and at  $t > 180$  minutes, current efficiencies are lower than the theoretical due to increased side reaction (Eq. 5). It is important to point out that the electrode potential, during the three electrolyses, was located in the potential range of  $2.4 \leq E \leq 2.9 \text{ V vs. SHE}$ , in order to avoid oxygen evolution reactions, which typically occurred at  $E > 2.9 \text{ V vs. SHE}$  [13].

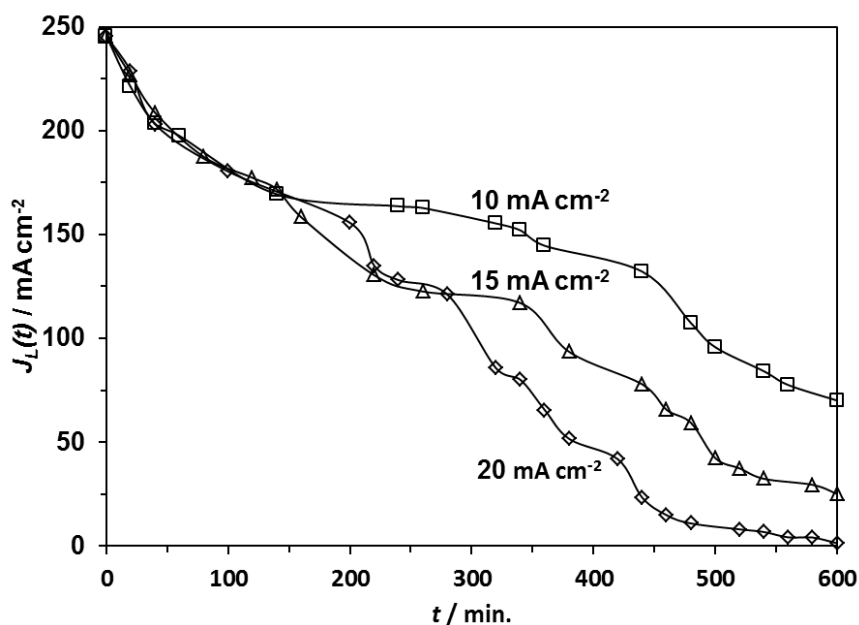


**Figure 4.** Influence of applied current density on theoretical limiting current density of electro combustion during the electrolysis of reactive blue 222, evaluated by means of equation (2) with the corresponding  $\text{COD}(t)$  values from the electrolyses similar to those in Figure 3.

Figure 4 shows the theoretical limiting current densities,  $J_L(t)$ , at any time of electrolysis, evaluated by means of equation (2) with the corresponding  $\text{COD}(t)$  values from the electrolyses similar to those in Figure 3. From the electrolysis at applied current density of  $10 \text{ mA cm}^{-2}$ , it can be observed that during the entire time of electrolysis  $J_L(t)$  present higher values than the applied current density,

indicating that the process never becomes limited by mass transport. The same behavior is obtained for the curve at applied current density of  $15 \text{ mA cm}^{-2}$ . However, at applied current density of  $20 \text{ mA cm}^{-2}$  (at  $t = 440$  minutes), the process is mass transport controlled, and then, at  $t > 440$  minutes, the applied current density value is higher than the following theoretical limiting current densities values. The above supports, omitting the obtained at applied current density of  $20 \text{ mA cm}^{-2}$  ( $t > 440$  minutes), that the experimental conditions applied herein avoid oxygen evolution reaction, which typically occurs at applied current densities values higher than the limiting current density.

From the analysis of Figure 3, it is observed that the oxidation rate is affected by current density, and is favored at  $20 \text{ mA cm}^{-2}$ , with current efficiency of 0.7 at the end of the electrolysis (100% COD removal). In order to compare the results obtained herein, it is important to mention that Panizza and coworkers reported the oxidation of a real textile effluent achieving current efficiency values of 0.35 (at  $20 \text{ mA cm}^{-2}$ , on BDD) [9]. In addition, the oxidation of reactive methyl orange at current densities of  $50 \text{ mA cm}^{-2}$  (on BDD) achieved values of current efficiency of 0.42 [10]. The best current efficiencies obtained herein are associated with the applied current densities, which were lower than limiting current density, and with the best mass transport performed in the FM01-LC reactor.

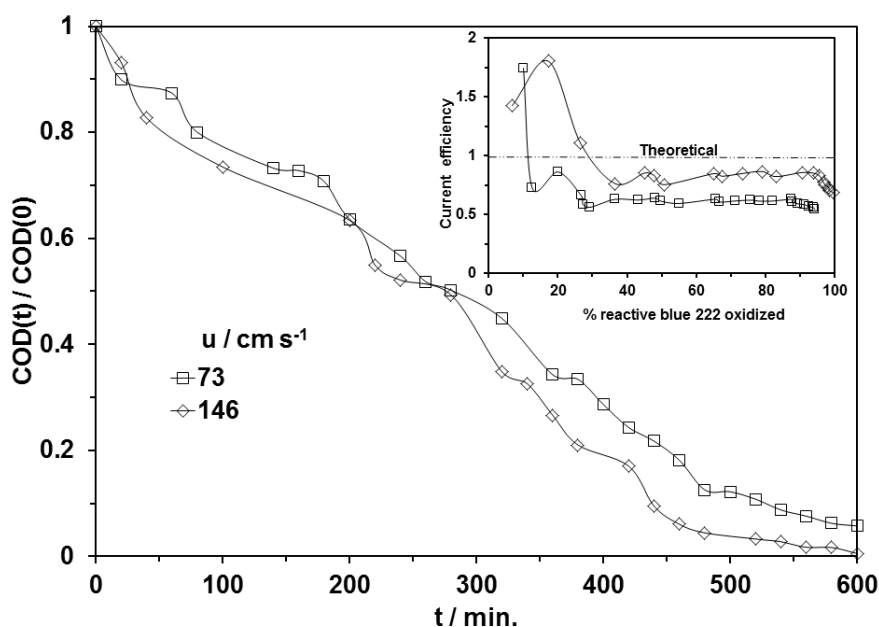


**Figure 5.** Influence of convection on the evolution of normalized COD and current efficiency (inset) during the electrolysis of reactive blue 222. Initial electrolyte:  $0.04 \text{ mol dm}^{-3}$  COD ( $1300 \text{ mg dm}^{-3} COD(0)$ ) in  $0.5 \text{ mol dm}^{-3} \text{ Na}_2\text{SO}_4$ ; the resulting solution exhibits a pH of 4.5,  $T=298 \text{ K}$ . Conditions:  $J = 20 \text{ mA cm}^{-2}$ ,  $A = 64 \text{ cm}^2$ . Mean linear flow velocities are shown in the Figure.

Figure 5 shows the depletion of COD during the reactive blue 222 electrochemical oxidation at mean linear flow velocity of  $73$  and  $146 \text{ cm s}^{-1}$ . As can be observed the COD trend present a slightly improvement with flow velocity due to the process is not limited by mass transport, as discussed above. It is important to mention that all of the electrolyses presented herein were developed in the

undivided FM01-LC reactor, for which reason the degradation of organics may also involve reactions at the cathode. The inset shows the current efficiency during reactive blue 222 electrochemical oxidation. Current efficiency surpasses unity (theoretical value) at the beginning of the electrolyses at the two flow velocities values, indicating that reactive blue oxidation by-products help the degradation itself, and it is improved at  $146 \text{ cm s}^{-1}$ . A similar behaviour was observed in previous studies, during *p*- and *o*- cresol mineralization processes in the same flow cell, at current densities comprised between  $5$ - $20 \text{ mA cm}^{-2}$  [13].

The energy consumption by electrolysis,  $E_c$ , for the electrolyses performed at  $20 \text{ mA cm}^{-2}$ , evaluated at 90% of degradation were  $14.1$  and  $11.8 \text{ KWh m}^{-3}$  for mean linear flow velocity of  $73$  and  $146 \text{ cm s}^{-1}$ , respectively. Equation 6 was employed for the estimation of energy consumption by electrolysis [13]:

$$E_c = \frac{4FE_{cell}}{\phi V_m} * \frac{1}{3.6} \quad (6)$$

Where  $E_{cell}$  is the cell potential in V, and  $V_m$  is the molar volume in  $\text{cm}^3 \text{ mol}^{-1}$ . The value of  $3.6$  is a correction factor which converts  $E_c$  to units of  $\text{KWh m}^{-3}$ .

Panizza and coworkers reported energy consumption of  $45 \text{ KWh m}^{-3}$  during the oxidation of a real textile effluent (at  $20 \text{ mA cm}^{-2}$ , on BDD) [9]. While, Zhou et al. achieved values of energy consumption of  $15.5 \text{ KWh m}^{-3}$  during the oxidation of reactive methyl orange at current densities of  $50 \text{ mA cm}^{-2}$  (on BDD) [10].

### 3.2 Detection and quantification of generated carboxylic acids

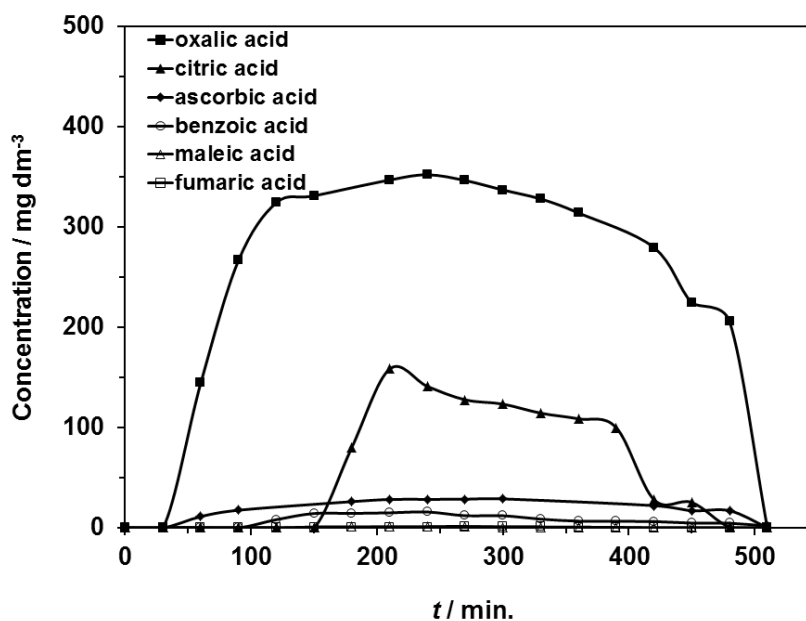


**Figure 6.** Evolution of carboxylic acids detected during the degradation of reactive blue 222 under the same condition of Figure 5 at  $u = 73 \text{ cm s}^{-1}$  and  $J = 20 \text{ mA cm}^{-2}$ .

HPLC chromatograms of the above degraded solutions exhibited the presence of peaks related to short-chain linear carboxylic acids formed during the destruction of reactive blue 222 by reaction with oxidants generated at the BDD anode (mainly  $\bullet\text{OH}$ ) at  $20 \text{ mA cm}^{-2}$  and  $u = 73$ . The retention time of the carboxylic acid were the following: oxalic ( $t_r = 1.4$  minutes), ascorbic ( $t_r = 2.2$  minutes), citric ( $t_r = 3.6$  minutes), fumaric ( $t_r = 3.9$  minutes), maleic ( $t_r = 4.4$  minutes), and benzoic ( $t_r = 13.6$  min).

Figure 6 shows that oxalic and citric acid are accumulated in high concentrations of  $324$  and  $160 \text{ mg dm}^{-3}$ , at  $120$  and  $210$  minutes of electrochemical oxidation, respectively. The content of citric acid drops slowly from  $140 \text{ mg dm}^{-3}$  at  $240$  minutes to close to  $1 \text{ mg dm}^{-3}$  at  $480$  minutes; while oxalic acid remains the major and persistent component in the solution. After  $300$  minutes of treatment, the concentration of oxalic acid starts to diminish to  $337 \text{ mg dm}^{-3}$ , although it is necessary to increase the treatment time at  $510$  minutes to achieve complete elimination of this specie. The complete degradation of ascorbic and benzoic acid, which are produced at low concentration ( $28$  and  $16 \text{ mg L}^{-1}$ , respectively,  $t = 240$  minutes), is achieved at  $510$  minutes of electrolysis. Maleic and fumaric acids are produced in very low concentrations ( $1 \text{ mg dm}^{-3}$ ) at  $120 \leq t \leq 420$  minutes, and are completely degraded after  $420$  minutes.

The maleic and fumaric acids are produced from the oxidative breakdown of the benzenic rings of aromatic byproducts, which are subsequently oxidized to oxalic acid [18, 19]. Oxalic acid is the ultimate carboxylic acid, with slow degradation kinetics, and is transformed directly into  $\text{CO}_2$ . The  $94\%$  COD removal of this electrolysis suggests the presence of intermediates which were not detected by this technique.

#### 4. CONCLUSIONS

Electrolysis studies indicated that the oxidation of reactive blue 222 was carried out via adsorbed hydroxyl radicals formed by the oxidation of water at the BDD surface. The applied current densities employed herein were  $10$ ,  $15$  and  $20 \text{ mA cm}^{-2}$ , which values were lower than the limiting current densities of electro combustion. The degradation rate is slightly improved with hydrodynamics.

Ion-exclusion chromatography experiments, performed during the electrolysis at  $20 \text{ mA cm}^{-2}$  and mean linear flow velocity of  $73 \text{ cm s}^{-1}$ , exhibited the presence of carboxylic acids (oxalic, citric, ascorbic, benzoic, maleic and fumaric) during the destruction of reactive blue 222 by reaction with oxidants generated at the BDD anode, mainly BDD( $\bullet\text{OH}$ ).

The electrolysis with BDD electrode at  $J = 20 \text{ mA cm}^{-2}$  and mean linear flow velocity of  $146$  was the only experiment that lead to  $100\%$  mineralization of reactive blue 222, with and energy consumption of  $11.8 \text{ kWh m}^{-3}$  and fractional integral current efficiency of  $0.7$ . This study suggests that anodic oxidation with a BDD electrode is an excellent method for the treatment of effluents contaminated with reactive blue 222.

#### ACKNOWLEDGEMENTS

The authors are grateful to CONACYT and CONCYTEG for the economic support via the projects FOMIX GTO-2011-C03-162757 and FOMIX GTO-2012-C04-195057.

## References

1. F. I. Hai, K. Yamamoto, K. Fukushi, *Crit. Rev. Env. Sci. Tech.*, 37 (2007) 315.
2. V. Prigione, V. Tigrini, C. Pezzella, A. Anastasi, G. Sanna, G.C. Varese, *Water Res.*, 4 (2008) 2911.
3. P. Cañizarez, F. Martínez, C. Jiménez, J. Lobato, M. A. Rodrigo, *Environ. Sci. Technol.*, 40 (2006), 6418.
4. A. Gürses, M. Yalcin, C. Dogar, *Waste. Manage.*, 22 (2002) 491.
5. J. W. Lee, S. P. Choi, R. Thiruvengkatachari, W. G. Shim, H. Moon, *Dyes Pigments*, 69 (2006) 196.
6. C. Fersi, L. Gzara, M. Dhahbi, *Desalination*, 185 (2005) 399.
7. T. H. Kim, C. Park, J. Yang, S. Kim, *J. Hazard. Mater.*, 112 (2004) 95.
8. H. Selcuk, *Dyes Pigments*, 64 (2005) 217.
9. C. A. Martínez-Huitl, E. Vieira dos Santos, D. Medeiros de Araújo, M. Panizza, *J. Electroanal. Chem.*, 674 (2012) 103.
10. M. Zhou, H. Sarkka and M. Sillanpaa, *Sep. Purif. Technol.*, 78 (2011) 2090.
11. B. Louhichi, N. Bensalash, A. Gadri, *Chem. Eng. Technol.*, 29 (2006) 944.
12. C. J. Brown, D. Pletcher, F. C. Walsh, J. K. Hammond, D. Robinson, *J. Appl. Electrochem.*, 22 (1992) 613.
13. J. L. Nava, F. Núñez, I. González, *Electrochim. Acta*, 52 (2007) 3229.
14. L. Gherardini, P. A. Michaud, M. Panizza, C. Comninellis, N. Vatisstas, *J. Electrochem. Soc.*, 148 (2001) D78.
15. M. Griffiths, C. Ponce de León, F. C. Walsh, *AIChE J.*, 51 (2005) 682.
16. American Public Health Association/American Water Works Association/Water Pollution Control Federation, *Standard methods for the examination of water and wastewater*, New York, 1995.
17. C. Comninellis, *Electrochim. Acta*, 39 (1994) 1857.
18. E. Guinea, C. Arias, P. L. Cabot, J. A. Garrido, R. M. Rodríguez, F. Centellas, E. Brillas, *Water Res.*, 42 (2008) 499.
19. M. A. Oturan, M. Pimentel, N. Oturan, I. Sirés, *Electrochim. Acta*, 54 (2008) 173.